Journal of Applied Polymer Science

Electrospinning Silica/Polyvinylpyrrolidone Composite Nanofibers

Toni E. Newsome, Susan V. Olesik
Department of Chemistry and Biochemistry, The Ohio State University, Columbus, Ohio
Correspondence to: S. V. Olesik (E-mail: olesik@chemistry.ohio-state.edu)

ABSTRACT: Small diameter nanofibers of silica and silica/polymer are produced by electrospinning silica/polyvinylpyrrolidone (SiO_2/PVP) mixtures composed of silica nanoparticles dispersed in polyvinylpyrrolidone solutions. By controlling various parameters, 380 ± 100 nm diameter composite nanofibers were obtained with a high silica concentration (57.14%). When the polymer concentration was low, "beads-on-a-string" morphology resulted. Nanofiber morphology was affected by applied voltage and relative humidity. Tip-to-collector distance did not affect the nanofiber diameter or morphology, but it did affect the area and thickness of the mat. Heat treatment of the composite nanofibers at 200°C crosslinked the polymer yielding solvent-resistant composite nanofibers, while heating at 465°C calcined and selectively removed the polymer from the composite. Crosslinking did not change the nanofiber diameter, while calcined nanofibers decreased in diameter (300 ± 90 nm) and increased in surface area to volume ratio. Nanofibers were characterized by scanning electron microscopy (SEM) and thermogravimetric analysis (TGA). © 2014 Wiley Periodicals, Inc. J. Appl. Polym. Sci. **2014**, *131*, 40966.

KEYWORDS: composites; crosslinking; electrospinning; nanostructured polymers

Received 9 February 2014; accepted 1 May 2014
DOI: 10.1002/app.40966

INTRODUCTION

The development of new nanomaterials continues to be a main interest in materials science and separation techniques. Among the methods used to fabricate nanomaterials, electrospinning is a simple and cost-effective technique which relies on repulsive electrostatic forces to produce nanofibers from a viscoelastic polymer solution or melt. Electrospun nanofibers have been used in a variety of applications, ranging from extractive sorbents[1,2] and sensors,[3] to drug delivery and tissue scaffolds.[4] By controlling various parameters during the electrospinning process, nanofibers which are up to meters in length can readily be produced with diameters in the range of 50–900 nm.[5] As a result, electrospinning provides a facile technique for the fabrication of nanomaterials possessing high surface area to volume ratio. Nanomaterials with smaller fiber diameters provide a higher surface area to volume ratio and thus would provide higher loading capacity and efficiency as a sorbents in extractions and separations.

Electrospinning typically utilizes a high molecular weight polymer to provide the chain entanglement required to keep the polymeric jet intact during the spinning process. As a result, the versatility of electrospun polymer nanofibers is restricted due to the limited functionalities that pure polymer nanofibers offer. Thus, various polymer blends and polymer/inorganic mixtures have been developed into multifunctional polymer/inorganic composite nanofibers which vastly expand the variety of functionalities capable of being produced via electrospinning.[5,6] Silica is a material of particular interest due to the presence of silanol groups capable of a wide range of interactions with other species, such as proton donor or acceptor interactions, dipole–dipole interactions, induced dipole interactions, and interactions based on dispersion forces.[7] Additionally, by incorporating inorganic fillers into organic fibers, nanocomposites combine the advantages of polymeric materials, such as light weight and flexibility, and inorganic materials, such as high mechanical strength, heat stability, and chemical stability.[8] For example, silica/polymer nanocomposites are ideal for a wide variety of applications, including biomedical devices, membranes, sensors, and as extractive sorbents and chromatographic supports with high adsorption capacity.[9–11] Production of electrospun nanofibers containing silica (SiO_2) has been accomplished by electrospinning a sol–gel solution, either with[12,13] or without[14] a polymer, and by electrospinning a polymer solution blended with silica particles.[8,15–18] In either case, the composite silica/polymer nanofibers can be calcined to selectively remove the polymer matrix.[15,17]

The sol-gel technique involves the hydrolysis of a metal alkoxide, such as tetraethyl orthosilicate (TEOS). While the sol–gel

Additional Supporting Information may be found in the online version of this article.

© 2014 Wiley Periodicals, Inc.

itself can be electrospun, the electrospinning solution is usually mixed with a polymer to achieve the molecule chain entanglement required to prevent the electrically driven jet from breaking up, thus maintaining a continuous jet.[19] In both cases, the solution can only be electrospun at a certain point during, not before or after, the sol–gel reaction. The major drawback of this approach is that the dynamic reaction in the electrospinning solution makes it difficult to precisely control of morphology and even chemical and physical properties of the resulting nanofibers. For example, nanofiber diameters vary dramatically with hydrolyzing time and thus with electrospinning time; even the window of time that the sol–gel electrospinning solution remains spinnable is variable and can be as short as ten minutes.[13,20] This variability creates technological challenges to be able to consistently utilize electrospun silica-based nanofibers obtained via the sol–gel approach in a given application.

Compared to sol–gel methods, a more facile and convenient way to produce silica-based electrospun nanofibers is by directly adding silica particles to a polymer solution. In this way, a silica-nanoparticle/polymer dispersion can be directly electrospun, which avoids the variability that is related to sol–gel hydrolyzing time. Various polymers have been used to create electrospun pure silica nanoparticle/polymer nanofibers, including polyvinylalcohol (PVA),[15] polyacrylonitrile (PAN),[16,17] poly(methyl methacrylate) (PMMA),[8] polyethylene oxide (PEO),[17,18] polyacrylamide (PAM),[17] and pol y(vinylidene fluoride) (PVDF).[21] The most critical challenge with this approach is the homogenous nanoscale dispersion of the inorganic particles in the polymeric electrospinning solution and within the resulting composite nanofibers. Most often this means that the polymer and SiO_2 NP must share a common solvent for homogenous dispersion throughout the nanofiber composite. Therefore, most work with silica/polymer nanocomposites uses water-soluble or alcohol-soluble polymers, such as PVA or PEO.[8] using water- or alcohol-insoluble polymers such as PAN often results in a heterogeneous dispersion of particles in the electrospun nanofibers due to particle agglomeration and only very low levels of nanoparticles (1–5 wt %) can be dispersed successfully.[16,22] Nevertheless, using a water-soluble polymer in the electrospinning solution results in a water-soluble mat of nanofibers, which limits the application of silica-based nanocomposites fabricated with this approach. To obtain silica-based nanofibers which are insoluble in water, as-spun nanofibers require additional crosslinking to render the polymer insoluble or heating to selectively remove the soluble polymer itself. Therefore, using the water/ alcohol-soluble polymer PVP to create electrospun silica/polymer composite nanofibers would be ideal to promote the homogenous dispersion of silica nanoparticles at high concentrations in the electrospun nanocomposite, but these as-spun nanofibers would need to be crosslinked or heated to make them insoluble for applications involving water. However, there are few reports of electrospun silica/PVP fibers which possess nanoscale diameters or are insoluble in water.

Recently, magnetic nanoparticles coated in silica have been electrospun with polyvinylpyrrolidone (PVP)[5]; using 0.64 μm silica-coated magnetic nanoparticles (MNPs), the smallest obtained fibers were sub-micron (0.66 μm) with a relatively low final MNP concentration (7 wt %). In another case, fibers have been electrospun using an electrospinning solution which combined PVP, TEOS, and silica particles (0.8 μm)[23]; however, the resulting fibers were micron-sized (~2.5 μm) and the fibrous morphology was not maintained after calcination. In neither of these instances was the PVP thermally crosslinked for solvent resistance, which would limit their use in certain applications.

Herein, we report an electrospinning method to produce composite silica/ polyvinylpyrrolidone (SiO_2/PVP) nanofibers through the use of silica nanoparticles dispersed in a polyvinylpyrrolidone solution. The purpose of this work was to produce the smallest diameter nanofibers possible while maintaining homogenous nanofiber morphology. Electrospinning parameters as well as thermal post-treatment parameters for crosslinking and calcination were evaluated. To the best of our knowledge, this is the first time that electrospun silica/polymer nanofibers have been reported utilizing only PVP and pure silica nanoparticles; it is the thinnest diameter silica nanoparticle/PVP nanofibers (380 nm) that have been obtained using this small of silica nanoparticles (250 nm) and at this high of final concentration (57 wt %) of silica. Additionally, it is the first time that any silica nanoparticle/PVP nanofibers have been crosslinked for solvent stability or calcined to remove the PVP matrix while maintaining nanofibrous morphology.

EXPERIMENTAL

Reagents

Silica nanoparticles (SiO_2 NPs), AngstromSphere monodispersed silica powder, 250 nm with a particle size standard deviation of <10%, were purchased from Fiber Optic Center Inc. (New Bedford, MA). The electrospinning polymer, polyvinylpyrrolidone (PVP), average M_w 1,300,000, K 85–95, was purchased from Acros Organics through Fisher Scientific (Pittsburgh, PA). Reagent alcohol (consists of 90% ethanol, 5% methanol, and 5% 2-propanol; HPLC grade, 99.8% purity), the solvent for the polymer solution and nanoparticle dispersion, was purchased from Fisher Scientific. Methanol was purchased from Macron Chemicals (St. Louis, MO).

Instrumentation

The apparatus used for electrospinning is described below. The composite SiO_2/PVP nanofibers were crosslinked using a Lindberg/Blue tube furnace (Model TF55030A, Waltham, MA) and were calcined using a Lindberg/Blue M tube furnace (Model STF55346C-1, Waltham, MA). The scanning electron microscopes (SEM) used to obtain images of the electrospun nanofibers included a Hitachi S-3400 SEM (Hitachi High Technologies America, Inc., Pleasonton, CA) and a Quanta 200 Series SEM (FEI Company, Hillsboro, OR). For the Hitachi S-3400 SEM, each electrospun sample was sputter coated with gold for 2 min at 10 μA to create a conductive surface for SEM imaging. Similarly, for the Quanta SEM, each sample was sputter coated with gold for 1 min at 15 μA. Digital images were taken with a Canon A650IS 12.1 MP digital camera. Thermogravimetric analysis (TGA) was performed using a TGA Q50 (TA Instruments, New Castle, DE).

Preparation of SiO_2/PVP Electrospinning Solutions

Polyvinylpyrrolidone solutions were prepared by dissolving PVP (9.0, 10.0, or 11.0 wt %) at room temperature. Silica nanoparticle dispersions were prepared by dispersing dry SiO_2 NPs in

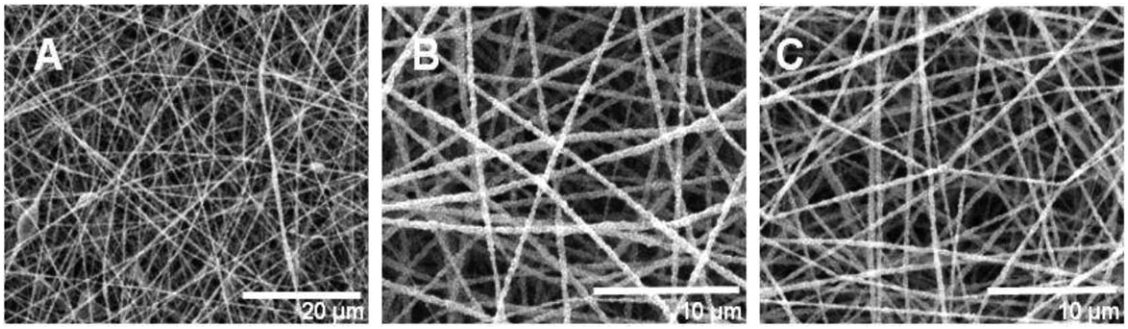

Figure 1. SEM images of electrospun SiO_2/PVP nanofibers using polymer solutions with different PVP concentrations of (a) 9.0 wt %, (b) 10.0 wt %, and (c) 11.0 wt % mixed with 20 wt % SiO_2 NPs at a 2:3 ratio (SiO_2 dispersion: PVP solution). All other electrospinning parameters were held constant (10 kV, 10 cm, 30 μL min^{-1}, RH < 50%). Images were taken with the Quanta 200 Series SEM.

the same solvent (20.0, 25.0, or 30.0 wt %). The dispersions were stirred for 2 h, sonicated for 3 h, and stirred overnight (≥12 h). These dispersions were sonicated again for at least 30 min prior to making the composite SiO_2/PVP electrospinning solutions. Electrospinning solutions were prepared by mixing the SiO_2 NP dispersion with the PVP solution at a 2:3 weight ratio (silica dispersion: PVP solution, respectively). These solutions were stirred for 2 h and sonicated for at least 4 h prior to electrospinning.

Optimization of Electrospinning Composite SiO_2/PVP Nanofibers

The electrospinning apparatus used in this experiment to produce composite SiO_2/PVP nanofibers is depicted in Figure S1 in the Supporting Information section. It included a Spellman CZE1000R high voltage power supply, ±0–30 kV (Spellman High Voltage Electronics Corporation, Hauppauge, NY); a Pump 11 Elite infusion only syringe pump (Harvard Apparatus, Holliston, MA); a digital hygrometer/thermometer probe (VWR, Radnor, PA); a spinneret consisting of a 10 mL plastic syringe equipped with a 23 GA blunt-end precision tip needle (Nordson EFD, Westlake, OH); and a 6.5 cm × 11.0 cm collector consisting of 0.003″ thick stainless steel (SS316) shim stock (McMaster-Carr, Aurora, OH). The tip of the spinneret, the collector, and the digital hygrometer/thermometer probe were placed inside of a custom-built acrylic electrospinning enclosure, 19″ × 24″ × 36″ (American Plastic Distributors, Columbus, OH); all other equipment was placed outside of the box. By using this enclosure, not only were the nanomaterials safely isolated during the electrospinning process, but also the humidity and temperature of the electrospinning environment could be monitored. All SEM images of the electrospun nanofibers were analyzed using ImageJ software (available from NIH at http://rsbweb.nih.gov/ij/).

RESULTS AND DISCUSSION

Effect of Polymer and Nanoparticle Concentration

This is the first reported example of electrospinning only PVP and pure silica nanoparticles. As such, all parameters related to the electrospinning process were studied and optimized to produce the smallest diameter nanofibers possible while maintaining homogenous nanofiber morphology. Two categories of variables affect nanofiber quality: materials variables, such as the polymer and solvent specifications, and process variables, such as the operating parameters including applied voltage, tip to collector distance, relative humidity, and feed rate.[5] Of these, one of the most critical factors in optimizing electrospun nanofibers is the concentration of the polymer and any additives in the electrospinning solution.[5] Using similar polymer and nanoparticle concentrations to those used by Lim et al.[17] with PEO and PAM in water, various PVP and silica nanoparticle concentrations were investigated with the goal of minimizing nanofiber diameter and maximizing the amount of inorganic nanoparticles within the nanofiber composite, while at the same time keeping a homogenous dispersion of nanoparticles within composite nanofibers.

Previous studies of electrospinning pure PVP using the same molecular weight (M_w 1,300,000 g mol^{-1}) reported that fiber formation began at around 3 wt % (fibers and beads) with the transition to fibers only occurring at around 7–9 wt % PVP.[24] Accordingly, polymer solutions with different concentrations of PVP (9.0, 10.0, and 11.0 wt %) were mixed with 20.0 wt % SiO_2 NP dispersions at a 2:3 weight ratio (SiO_2 dispersion: PVP solution); this resulted in electrospinning solutions with final PVP concentrations of 5.4, 6.0, and 6.6 wt % and a SiO_2 concentration of 8.0 wt %. Figure 1 shows SEM images of the resulting composite nanofibers. The nanofibers from the 9.0 wt % PVP solution contain morphological deformities such as beads [Figure 1(a)]. Beads, the most common defect encountered in electrospinning, were a result of the surface tension forces overcoming the forces which favor continuous jet elongation.[5] This "beads on a string" morphology can be eliminated by increasing the concentration of polymer in the solution to allow for adequate chain entanglement and promote continuous jet elongation. As such, the nanofibers from both the 10.0 and 11.0 wt % PVP solution do not contain beads, [Figure 1(b,c), respectively]. Additionally, the nanofibers resulting from the 9.0 and 10.0 wt % PVP solution have a smaller average nanofiber diameter than those resulting from the 11.0 wt % solution (380 nm compared to 430 nm, respectively), because higher polymer concentrations typically yield nanofibers with larger average diameters.[19] Therefore, 10.0 wt % was determined to be the optimum concentration of PVP as it produced the smallest diameter nanofibers without bead deformity, and all remaining experiments utilize electrospinning solutions made from this concentration of PVP.

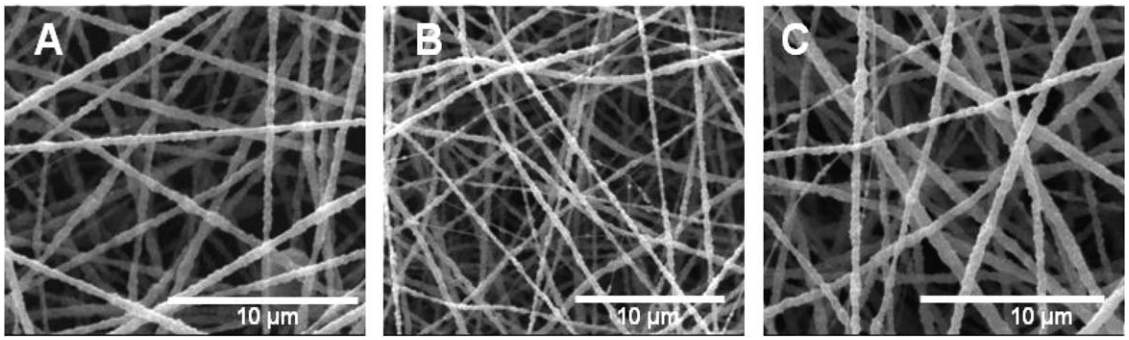

Figure 2. SEM images of electrospun SiO_2/PVP nanofibers using SiO_2 dispersions with different SiO_2 concentrations of (a) 20.0 wt %, (b) 25.0 wt %, and (c) 30.0 wt % mixed with 10.0 wt % PVP at a 2:3 ratio (SiO_2 dispersion: PVP solution). All other electrospinning parameters were held constant (10 kV, 10 cm, 30 μL min^{-1}, RH<50%). Images were taken with the Quanta 200 Series SEM.

Similarly, the effect of nanoparticle concentration on the electrospun composite nanofibers was investigated by making SiO_2 NP dispersions at 20.0, 25.0, and 30.0 wt % and mixing with 10.0 wt% PVP at a 2:3 ratio (SiO_2 dispersion: PVP solution); this resulted in electrospinning solutions with final SiO_2 concentrations of 8.0, 10.0, and 12.0 wt % and an optimized PVP concentration of 6.0 wt %. Increasing the SiO_2 concentration from 20.0 to 25.0 wt % yielded more heterogeneous nanofibers in that there were an increasing number of nanofibers with large distances between nanoparticles [Figure 2(a,b), respectively]. This is less of an issue with the nanofibers from the 20.0 or 30.0 wt % SiO_2 dispersions [Figure 2(a,c), respectively]. Similar to increasing polymer concentration, increasing silica nanoparticle concentrations also resulted in increasing average nanofiber diameters, as demonstrated in Figure 3, where nanofibers resulting from the 20.0 wt % dispersion had a smaller average diameter than those resulting from the 30.0 wt % dispersion (380 nm compared to 540 nm, respectively). The increase in fiber diameters was a result of increasing solution viscosity from the additional silica content. Thus, to maximize the silica content while maintaining thin and homogenous fibers, 20.0 wt % was determined to be the optimum concentration of SiO_2 NPs as this concentration produced the smallest diameter nanofibers with homogenous nanoparticle dispersion, and all remaining experiments utilize electrospinning solutions made from this concentration of SiO_2.

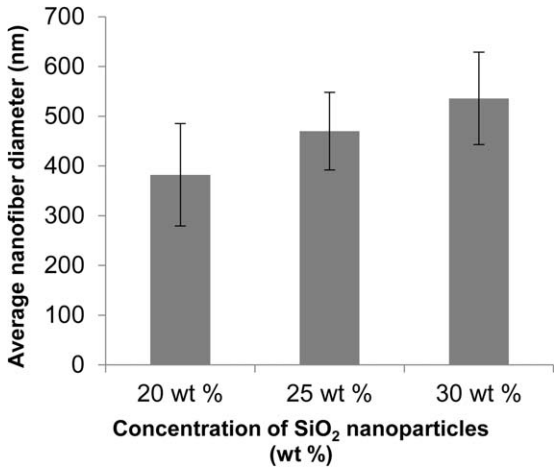

Figure 3. The effect of the concentration of SiO_2 NPs on average nanofiber diameter. The composite nanofibers were electrospun using SiO_2 dispersions with different SiO_2 concentrations of 20.0, 25.0, and 30.0 wt % mixed with 10.0 wt % PVP at a 2:3 ratio (SiO_2 dispersion: PVP solution). All other electrospinning parameters were held constant (10 kV, 10 cm, 30 μL min^{-1}, RH < 50%).

Effect of Applied Voltage

The applied voltage is critical in electrospinning. The high voltage induces charges on the solution which are necessary in initiating electrospinning as the surface tension is overcome by the electrostatic forces in the solution.[6] Typically, a positive or negative applied voltage of 6 kV is sufficient to draw fibers from the electrospinning solution.[19] As a result, the applied voltage had a large effect on both nanofiber morphology and diameter as depicted in Figure 4. Nanofiber diameter increases from 350 nm to 380 nm to 450 nm with increasing applied voltage (+8, +10, and +12 kV, respectively). In most cases, a higher applied voltage leads to greater stretching of the polymer jet due to the greater columbic forces and stronger electric field, which results in thinner fiber diameter.[6,19,25] However, in other cases, lower voltages result in a decrease in fiber diameter due to the reduced acceleration of the jet and weaker electric field, which increases the time of flight of the jet allowing for more fiber stretching.[19,26,27] In such instances, to obtain thinner fibers, voltages closer to the critical voltage would be advantageous. At applied voltages lower than 8 kV, electrospraying occurs, while at an applied voltage of 8 kV, near the critical voltage, the "beads on a string" morphology is observed. 10 kV was thus chosen as the optimum applied voltage for thinnest nanofiber diameter with a bead-free morphology.

Effect of Flow rate, Relative Humidity, and Tip to Collector Distance

Other controllable electrospinning parameters include flow rate, tip to collector distance, and relative humidity. The flow rate determines how much of the electrospinning solution is available at the tip of the spinneret for fiber formation. For a given voltage, there is a lower limit of flow rate for the Taylor cone to be stabilized.[19] Increasing the flow rate above this increases fiber diameter because there is a greater volume of solution able to be drawn from the spinneret tip. Flow rates between 15 and 30 μL min^{-1} were studied. Because the flow rates examined had

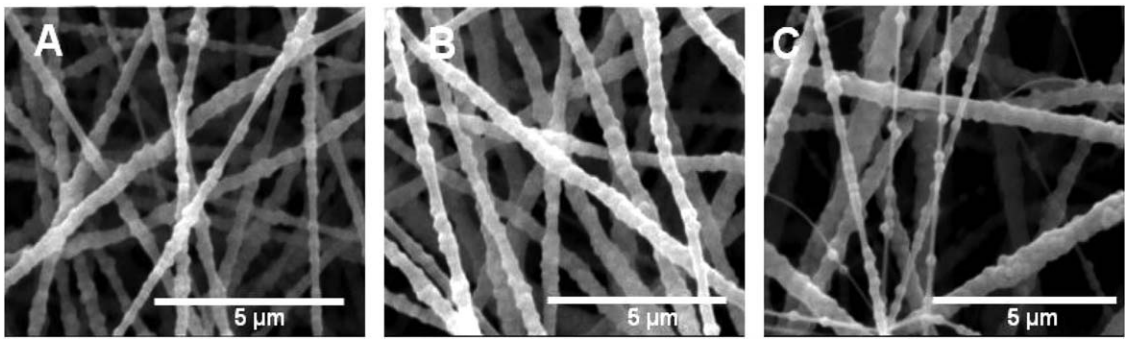

Figure 4. SEM images of electrospun SiO_2/PVP nanofibers using various applied voltages of (a) 8 kV, (b) 10 kV, and (c) 12 kV. All other electrospinning parameters were held constant (2:3 ratio of 20.0 wt % SiO_2: 10.0 wt % PVP, 10 cm, 30 μL min^{-1}, RH<50%). Images were taken with the Quanta 200 Series SEM.

no noticeable effect on the morphology or significant difference on average nanofiber diameter, 15 μL min^{-1} was determined to be the optimum flow rate.

Relative humidity (RH) of the electrospinning environment influences the rate of evaporation of the solvent in the electrospinning jet.[19] While the range of relative humidity (0–55%) examined had little effect on the overall morphology or average nanofiber diameter, some bead formation was observed at a RH above 50%. This effect has previously been observed in electrospinning of pure PVP nanofibers.[28,29] At increased relative humidity with higher ambient water levels, PVP nanofiber diameter often decreases because the fluid PVP jet has a decreased solvent evaporation rate, allowing the charged jet more time to continue to elongate during electrospinning.[30] At the same time, the charge per unit area decreases as the surface area increases. Therefore, if the relative humidity is too high, jet instability is developed and beaded nanofibers are formed as the surface tension forces in the jet overcome the forces promoting jet elongation.[30] For the SiO_2/PVP nanofibers, jet instability was observed at relative humidity levels above 50%. Thus, all electrospun samples were fabricated using ambient conditions as long as the RH remained at or below 50%.

Varying the tip to collector distance influences the flight time of the polymer fiber. For successful fiber collection, the electrospinning polymer jet must have sufficient time for solvent evaporation to occur during its flight; otherwise, fibers may fuse or puddle on the collector. At all distances examined (10–20 cm), the fibers produced do not fuse together on the collector, which suggests that 10 cm was sufficient flight time for solvent evaporation or occur. The tip to collector distance had no significant effect on the average nanofiber diameter or morphology at the nanoscale. However, on the macroscale, it does change the area and thickness of the collected nanofibrous mat. Using a distance of 10 cm produced nanofiber mats which were only about 4 cm × 4 cm in size, as compared to those produced at 15 cm which covered the entire collector (6.5 cm × 11.0 cm). Using a distance of 20 cm produced mats which also covered the entire collector, but they were visibly thinner than those produced at 15 cm at the same given collection time. The increase in the area of the collected mat, or deposition area of the nanofibers, can be understood by considering the whipping instability region of the nanofibers during electrospinning. During the electrospinning process, the jet of polymer fibers which is ejected from the tip of the spinneret is initially straight. To reduce the density of surface charges, the initially straight jet becomes instable and begins to bend to promote jet extension and increase surface area [5]. This whipping instability region of the polymer jet takes on a conical shape around the axis of the straight segment. As a result, when the collector is placed perpendicular to the tip of the spinneret, the shape of the deposited nanofiber mat is typically circular like the base of a cone because the collector intersects the cone of the polymer jet. At a given distance between the tip of the spinneret and the collector, the deposited mat is circular when the collector area is larger than the area of the base of the conical polymer jet. When the collector is smaller than the base of the polymer jet, the deposited mat of fibers tends to wrap around the collector. If the distance between the tip of spinneret and the collector is increased, the collector intersects the cone of the nanofiber jet at a longer distance and therefore the base of the conical polymer jet is larger. This results in a mat of fibers with a larger deposited area. At this longer distance, if the nanofibers are being electrospun at the same rate but over a larger deposition area, the thickness of the collected nanofiber mat will naturally be thinner at a given collection time compared to shorter distances. Therefore, the tip to collector distance should be carefully considered depending on the application intended as the selected distance will affect the area and thickness of the electrospun mat of nanofibers obtained through this method, but it will not affect the average nanofiber diameter or morphology.

Optimization of Thermal Crosslinking Conditions

PVP is soluble in water and many alcohols, which limits the applicability of electrospun PVP-based nanofibers if left as-spun. While PVP is known to decrease in solubility upon heating in air between 150 and 200°C,[31,32] few reports of electrospun PVP or PVP composites utilize thermal crosslinking.[33] The as-spun SiO_2/PVP nanofibers were crosslinked in a tube furnace at low relative temperatures under constant air flow (140 mL min^{-1}) to investigate the effect thermal crosslinking on solvent stability. To the best of our knowledge, this is the first report of thermally crosslinking electrospun PVP with SiO_2 NPs to obtain insoluble composite SiO_2/PVP nanofibers. As such, the final

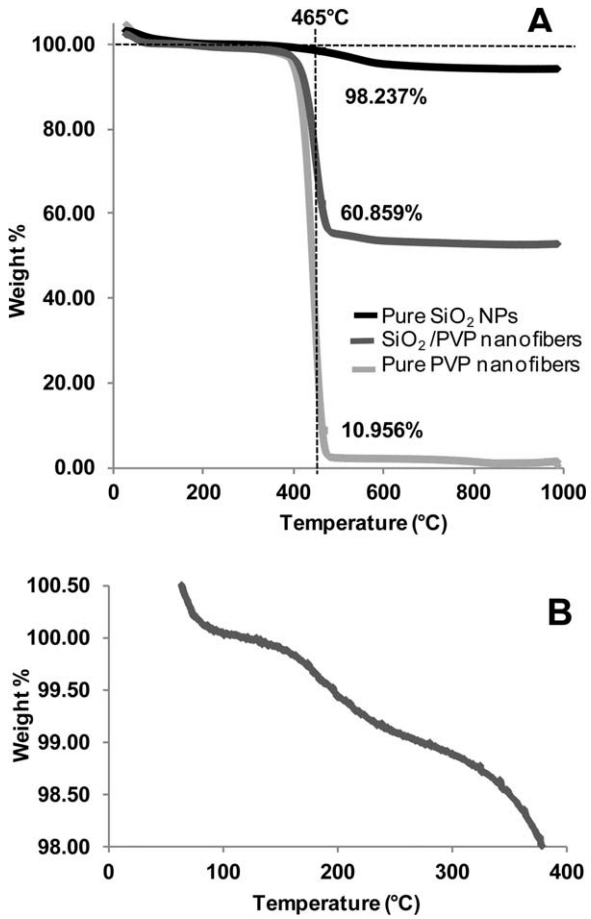

Figure 5. (a) TGA curves of pure SiO_2 nanoparticles (black), pure electrospun PVP nanofibers (light gray), and composite SiO_2/PVP nanofibers (dark gray) and (b) a magnified view of the TGA curve of the composite SiO_2/PVP nanofibers in the region used for thermal crosslinking.

temperature in the thermal crosslinking heat program was investigated to minimize the solubility of SiO_2/PVP nanofibers.

To identify the appropriate temperature range for thermal crosslinking, the as-spun SiO_2/PVP nanofibers were characterized by thermal gravimetric analysis (TGA), using pure SiO_2 NPs and pure PVP for comparison. The results are presented in Figure 5. All three initially exhibited weight loss before 100°C which was attributed to water adsorption; the weight percentages on the TGA curves were corrected for this initial weight loss. In both the pure PVP nanofibers and in the SiO_2/PVP nanofibers, a second weight loss occurs between 150 and 200°C, which can be seen in the inset of Figure 5 for the SiO_2/PVP nanofibers. This suggested that thermal crosslinking of the PVP polymer occurs in this temperature range, which was in good agreement with previously reported thermal crosslinking temperatures for other composite PVP materials.[31,32] Finally, there was significant weight loss between 350 and 470°C accounting for the decomposition of PVP.

In the optimization of the thermal crosslinking temperature program, final temperatures of 125, 150, 175, and 200°C were investigated as thermal crosslinking was noted to occur between 150 and 200°C, as mentioned above. The as-spun SiO_2/PVP nanofibers were heated in air to the specified final temperature at 2°C min^{-1} and held overnight. After thermal treatment, the nanofibers were immersed in solvents typical of untreated PVP (water, methanol, and ethanol). The solubility and resulting fibrous morphology of the thermally treated nanofibers were examined and compared to the solvent stability of the untreated as-spun SiO_2/PVP nanofibers. Figure 6 shows SEM images of the as-spun and thermally treated SiO_2/PVP nanofibers both before and after immersion in water. As expected, both the non-treated (as-spun) nanofibers and nanofibers heated to 125°C dissolved in water, methanol, and ethanol [Figure 6(f,g), respectively]. Nanofibers which were heated to 150 and 175°C did not completely dissolve in water; however much of the fibrous morphology was lost for nanofibers heated to 150°C [Figure 6(h)] and those heated to 175°C maintained nearly all morphology but nanofiber swelling was observed [Figure 6(i)]. Thermal crosslinking appears to be complete for nanofibers heated to 200°C as there was no observed swelling or difference in nanofiber morphology.

To identify the temperature at which crosslinking occurs more specifically, additional final temperatures of 180, 185, 190, and 195°C were investigated and compared to those heated to 175 and 200°C. SEM images of the thermally treated SiO_2/PVP nanofibers after immersion in water can be found in Supporting Information Figure S2. Nanofibers which were heated to 180 and 185°C maintained nearly all morphology but nanofiber swelling was observed [Supporting Information Figure S2(b,c)]. Thermal crosslinking appears to be complete for nanofibers heated to 190 and 195°C as there was no observed swelling or difference in morphology [Supporting Information Figure S2(d,e)]. To ensure complete thermal crosslinking which maintained nanofibrous morphology without fiber swelling, the optimum final temperature was determined to be 200°C. Additionally, there was no significant difference in average diameter for the nanofibers processed at these thermal crosslinking temperatures compared to the as-spun nanofibers. A complete summary of the results for all investigated final temperatures can be found in Table I.

Optimization of Calcination Conditions

Higher processing temperatures were also investigated such that the as-spun SiO_2/PVP nanofibers were calcined to remove the polymer matrix.[15,17] Various final temperatures (350, 400, 450, 465, 475, and 500°C), ramp rates (0.5, 1.0, 2.0, 5.0°C min^{-1}), and hold times (2, 4, 6, and 8 h) were considered in order to maximize the amount of PVP removed from the nanofibers while still maintaining a certain level of robustness in the mat for further use.

According to the TGA data shown in Figure 5, PVP begins to decompose at 350°C and continues to until complete removal at 470°C.[34] As such, final calcination temperatures of 350, 400, 450, 465, 475, and 500°C were investigated. As shown in Figure 7, close-packed SiO_2 NP nanofibrous structures remained after calcination. Even at the lowest final temperature examined (350°C), degradation of PVP was apparent; the nanofibers took on a rougher, more textured morphology as the polymer was removed and the SiO_2 NPs were exposed [Figure 7(a)], as

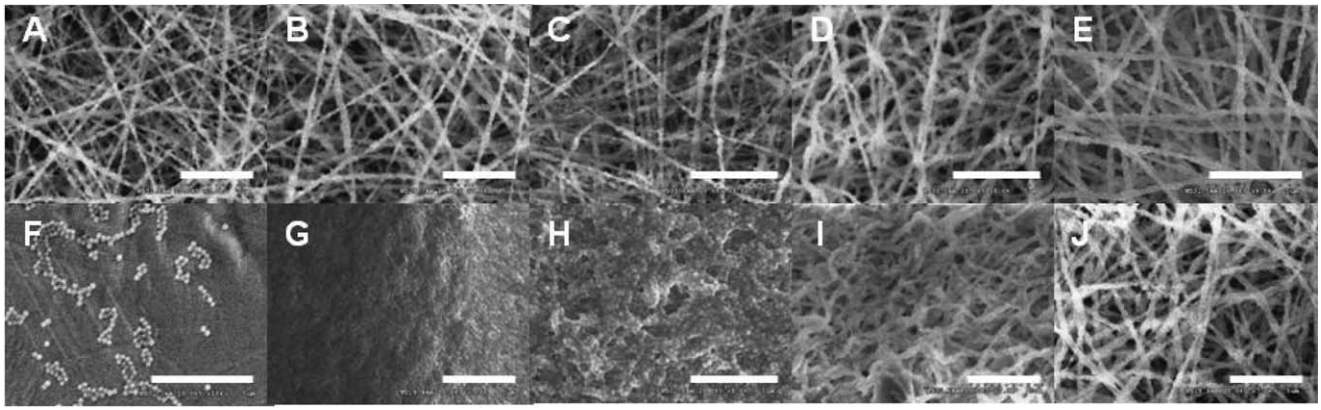

Figure 6. SEM images of electrospun SiO_2/PVP nanofibers thermally crosslinked using different final temperatures. Images (a–e) are after thermal treatment and (f–j) are after immersion in water overnight and dried. Final temperatures displayed here are (a,f) no treatment, (b,g) 125°C (c,h) 150°C, (d,i) 175°C, and (e,j) 200°C. Scale bars are 5 μm. Images were taken with the Hitachi S-3400 SEM.

compared to the smoother morphology of the as-spun nanofibers [Figure 4(b)]. At all of the final temperatures examined, the fibrous morphology of the electrospun samples was maintained after calcination. Guo et al. reported electrospinning silica/PVP composite fibers with tetraethylorthosilicate, however these micron-sized fibers did not maintain fibrous morphology after calcining.[23] In addition, the nanofibers heated to final temperatures of 475 and 500°C appeared to be more densely packed [Figure 7(e,f), respectively] than the nanofibers heated to lower final temperatures. The apparent density increase was confirmed by weighing a given area of nanofibers processed to different final temperatures. The density of the nanofiber mats increases with increasing final temperature. Nanofiber mats processed at 465°C were over five times denser than the as-spun nanofiber mats and were 30% denser than the mats processed at 350°C. Also, mats processed to 475 and 500°C appeared whiter and were much more brittle. This can be attributed to more of the polymer matrix being removed from these nanofibers at higher final temperatures, and should be carefully considered when choosing a final calcination temperature for these materials in a given application.

Nanofibers were calcined to final temperatures of 450, 465, 475, and 500°C using ramp rates of 0.5, 1.0, 2.0, and 5.0°C min^{-1}. Compared to higher ramp rates, using lower ramp rates (0.5°C min^{-1}) kept the calcined mats relatively flat and free from fracture (one large piece rather than many small pieces). Mats calcined to a final temperature of 450°C had 36.363% of PVP remaining in the nanofiber composite according to the TGA data in Figure 5 and they were quite dark compared to mats processed at higher final temperatures as a result of the left over polymer. Mats calcined to a final temperature of 475°C had 3.256% of PVP residue remaining in the nanofiber composite, however the nanofibers were so brittle that they broke down to silica nanoparticles upon minimum handling or contact with solvent. Therefore, optimum calcination parameters were determined to be a final temperature of 465°C and a ramp rate of 0.5°C min^{-1}. With 10.956% of the polymer remaining in the composite, these selected conditions provided nanofibrous mats which had the most amount of polymer removed without leaving the calcined material too brittle for use in a further application which required a contiguous mat. When calcining to 465°C at 0.5°C min^{-1}, a hold time of 6 h proved to be sufficient.

Table I. Summary of Solvent Stability and Morphological Observations for SiO_2/PVP Nanofibers Thermally Crosslinked at Different Final Temperatures

Final temperature (°C)	Solubility[a]	SEM observations	Crosslinked
No treatment (As-Spun)	Soluble	Only NPs left	No
125	Soluble	Only NPs left	No
150	Insoluble	Thin film with some fibrous morphology maintianed	Not complete
175	Insoluble	Morphology maintained; swelling	Not complete
180	Insoluble	Morphology maintained; swelling	Not complete
185	Insoluble	Morphology maintained; some swelling	Not complete
190	Insoluble	Morphology maintained; no swelling	Yes
195	Insoluble	Morphology maintained; no swelling	Yes
200	Insoluble	Morphology maintained; no swelling	Yes

[a] Solubility tested in three solvents: water, methanol, and ethanol.

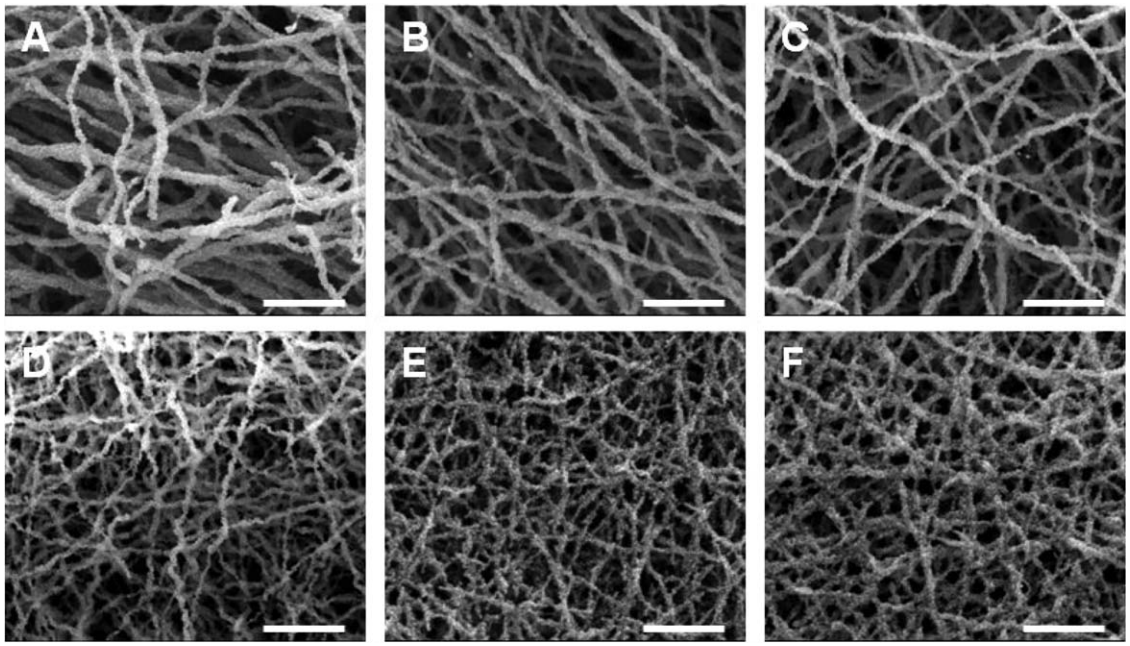

Figure 7. SEM images of calcined SiO_2/PVP nanofibers processed at different final temperatures of (a) 350°C, (b) 400°C, (c) 450°C, (d) 465°C, (e) 475°C, and (f) 500°C. Ramp rate was 2°C min^{-1} and the final temperature was held for 8 h. Optimized electrospinning parameters were used. Scale bars are 5 μm. Images were taken with the Quanta 200 Series SEM.

To determine the amount of PVP and SiO_2 NPs in the calcined nanofibers, TGA was performed with pure electrospun PVP nanofibers and pure SiO_2 NPs as well as the composite SiO_2/PVP nanofibers. Considering the initial concentrations of PVP and SiO_2 NPs in the composite electrospinning solution (6 and 8 wt %, respectively), the electrospun composite nanofibers consisted of 42.86% PVP and 57.14% SiO_2 after complete solvent evaporation. According to the TGA data in Figure 5, 10.956% of pure PVP nanofibers remained at 465°C; at this same temperature, 98.237% of pure SiO_2 NPs remained. Combining the TGA data of pure PVP and pure SiO_2 NPs with the initial concentrations of PVP and SiO_2 NPs in the as-spun composite nanofibers, 4.695% of PVP and 56.136% of SiO_2 NPs remained in the nanofibers at 465°C. This correlated to a combined 60.831% of PVP and SiO_2 NPs in the composite nanofibers remaining as the calcined nanofibers after heating to 465°C. Examination of the TGA data of the composite SiO_2/PVP nanofibers confirmed that 60.859% of the composite fibers remained at 465°C. Thus, the final calcined SiO_2/PVP nanofibers processed to 465°C consisted of 7.719% of PVP and 92.281% of SiO_2 (Figure S3in Supporting Information).

Table II. Average Nanofiber Diameter and BET Surface Area of As-Spun, Crosslinked, and Calcined SiO_2/PVP Nanofibers

SiO_2/PVP nanofiber	Nanofiber diameter (nm)	BET surface area (m^2 g^{-1})
As-spun	380 ± 100	10.7
Crosslinked	380 ± 110	9.84
Calcined	300 ± 90	7.49

Finally, SiO_2/PVP nanofiber diameters and surface areas were compared between the as-spun, crosslinked, and calcined nanofibers (Table II). The Brunauer–Emmett–Teller (BET) method was used to calculate the surface area of the different nanofiber types. The as-spun SiO_2/PVP nanofibers had an average nanofiber diameter of 380 nm and BET surface area of 10.7 m^2 g^{-1}. Thermal crosslinking did not change the average nanofiber diameter or BET surface area significantly. Upon polymer removal by calcination, the average nanofiber diameter decreased by ~20% (Figures S4 and S5 in the Supporting Information). This decrease in average nanofiber diameter resulted in the slight decrease in BET surface area as more of the polymer was removed from the composite. Considering that the density of the calcined nanofibers was approximately five times higher as discussed earlier, the surface area per volume of the calcined nanofibers was ~3.6 times greater than the as-spun nanofibers. The superior surface area to volume ratio of the calcined nanofibers could likely result in enhanced chemical or physical properties and improvements in the efficiency of this material when utilized as a sorbent in separations or in chemical delivery.

CONCLUSIONS

In summary, this work describes an optimized electrospinning method to produce composite SiO_2/PVP nanofibers through the use of pure silica nanoparticles dispersed in PVP solutions. Electrospinning conditions optimized to produce the smallest diameter fibers possible resulted in as-spun SiO_2/PVP nanofibers with an average nanofiber diameter of 380 nm and a high final concentration of silica (57 wt %) in the nanocomposite. Because they are water and alcohol soluble, these nanofibers could be useful as sorbents in organic-based extractions. The as-spun SiO_2/PVP nanofibers were thermally crosslinked at

200°C resulting in solvent-resistant SiO_2/PVP nanofibers. The solvent-resistance and flexibility of the crosslinked nanofibers makes them ideal in aqueous environments for drug delivery, as tissue scaffolds, or in water filtration. Calcining SiO_2/PVP nanofibers at 465°C resulted in selective removal of a majority of the PVP in the composite nanofibrous mat. The solvent resistant calcined nanofibers were composed of 7.719% of PVP and 92.281% of SiO_2 and had an average nanofiber diameter of 300 nm. The high surface area to volume ratio and solvent resistance of the calcined nanofibers would be beneficial when utilized as highly efficient sorbents in extractions and separations or in sensors.

ACKNOWLEDGMENTS

The authors thank the U.S. National Science Foundation for financial support of this research under grant CHE-1012279 and the undergraduate students who assisted in SEM image analyses, Chris Brue and Danielle Hopping, and Michael Severance in his assistance in acquiring BET surface area data.

REFERENCES

1. Zewe, J. W.; Steach, J. K.; Olesik, S. V. *Anal. Chem.* **2010**, *82*, 5341.
2. Newsome, T. E.; Zewe, J. W.; Olesik, S. V. *J. Chromatogr. A* **2012**, *1262*, 1.
3. Liu, H.; Kameoka, J.; Czaplewski, D. A.; Craighead, H. G. *Nano Lett.* **2004**, *4*, 671.
4. Buschle-Diller, G.; Hawkins, A.; Cooper, J. In Modified Fibers with Medical and Specialty Applications; Edwards, J. V.; Buschle-Diller, G.; Goheen, S. C., Eds.; Springer: Netherlands, **2006**; Chapter *5*, p 67.
5. Andrady, A. Science and Technology of Polymer Nanofibers; Wiley: Hoboken, New Jersey, **2008**.
6. Chen, M.; Qu, H.; Zhu, J.; Luo, Z.; Khasanov, A.; Kucknoor, A. S.; Haldolaarachchige, N.; Young, D. P.; Wei, S.; Guo, Z. *Polymer* **2012**, *53*, 4501.
7. Reich, E.; Schibli, A. High-Performance Thin-Layer Chromatography for the Analysis of Medicinal Plants; Thieme Medical Publishers: New York, NY, **2007**; Chapter *2*, p 22.
8. Chen, Y.; Zhang, Z.; Yu, J.; Guo, Z. *J. Polym. Sci. B Polym. Phys.* **2009**, *47*, 1211.
9. Keyur, D.; Kit, K.; Li, J. J.; Zivanovic, S. *Biomacromolecules* **2008**, *9*, 1000.
10. Shao, C.; Kim, H.; Gong, J.; Lee, D. *Nanotechnology* **2002**, *13*, 635.
11. Sawicka, K. M.; Gouma, P. *J. Nanopart. Res.* **2006**, *8*, 769.
12. Roh, S. H.; Lee, Y. A.; Lee, J. W.; Kim, S. I. *J. Nanosci. Nanotechnol.* **2008**, *8*, 5147.
13. Wen, S.; Liu, L.; Zhang, L.; Chen, Q.; Zhang, L.; Fong, H. *Mater. Lett.* **2010**, *64*, 1517.
14. Choi, S. S.; Lee, S. G.; Im, S. S.; Kim, S. H.; Joo, Y. L. *J. Mater. Sci. Lett.* **2003**, *22*, 891.
15. Kanehata, M.; Ding, B.; Shiratori, S. *Nanotechnology* **2007**, *18*, 315602.
16. Ji, L.; Saquing, C.; Khan, S. A.; Zhang, X. *Nanotechnology* **2008**, *19*, 085605.
17. Lim, J.; Moon, J. H.; Yi, G.; Heo, C.; Yang, S. *Langmuir* **2006**, *22*, 3445.
18. Sharma, N.; McKeown, S. J.; Ma, X.; Pochan, D. J.; Cloutier, S. G. *ACS Nano* **2010**, *4*, 5551.
19. Ramakrishna, S.; Fujihara, K.; Teo, W. E.; Lim, T. C.; Ma, Z. An Introduction to Electrospinning and Nanofibers; World Scientific Publishing Co.: Singapore, **2005**; Chapter *3*, p 90.
20. Ma, Z.; Ji, H.; Teng, Y.; Dong, G.; Tan, D.; Guan, M.; Zhou, J.; Xie, J.; Qiu, J.; Zhang, M. *J. Mater. Chem.* **2011**, *21*, 9595.
21. Kim, Y. J.; Ahn, C. H.; Lee, M. B.; Choi, M. S. *Mater. Chem. Phys.* **2011**, *127*, 137.
22. Ji, L.; Zhang, X. *Mater. Lett.* **2008**, *62*, 2165.
23. Guo, A.; Liu, J.; Dong, X.; Liu, M. *Mater. Lett.* **2013**, *95*, 74.
24. Shenoy, S. L.; Bates, W. D.; Frisch, H. L.; Wnek, G. E. *Polymer* **2005**, *46*, 3372.
25. Lee, J. S.; Choi, K. H.; Ghim, H. D.; Kim, S. S.; Chun, D. H.; Kim, K. Y.; Lyoo, W. S. *J. Appl. Polym. Sci.* **2004**, *93*, 1638.
26. Steach, J. K.; Clark, J. E.; Olesik, S. V. *J. Appl. Polym. Sci.* **2010**, *118*, 405.
27. Zhao, S. L.; Wu, X. H.; Wang, L. G.; Huang, Y. *J. Appl. Polym. Sci.* **2004**, *91*, 242.
28. Yuya, N.; Kai, W.; Kim, B. S.; Kim, I. S. *J. Mater. Sci. Eng. Adv. Technol.* **2010**, *2*, 97.
29. Vrieze, S. D.; Camp, T. V.; Nelvig, A.; Hagstrom, B.; Westbroek, P.; Clerck, K. D. *J. Mater. Sci.* **2009**, *44*, 1357.
30. Tripatanasuwan, S.; Zhong, Z.; Reneker, D. H. *Polymer* **2007**, *10*, 5742.
31. Borodko, Y.; Habas, S. E.; Koebel, M.; Yang, P.; Frei, H.; Somorjai, G. A. *J. Phys. Chem. B* **2006**, *110*, 23052.
32. Yoshida, M.; Prasad, P. N. *Appl. Opt.* **1996**, *35*, 1500.
33. Jin, M.; Zhang, X.; Nishimoto, S.; Liu, Z.; Tryk, D. A.; Murakami, T.; Fujishima, A. *Nanotechnology* **2007**, *18*, 075605.
34. Peniche, C.; Zaldívar, D.; Pazos, M.; Páz, S.; Bulay, A.; San Román, J. *J. Appl. Polym. Sci.* **1993**, *50*, 485.